Systems of Hydrodynamic Type
that Approximate Two-Dimensional Ideal Fluid Equations

V. P. Dymnikov[a], * and P. A. Perezhogin[a], *

[a]Institute of Numerical Mathematics, Russian Academy of Sciences, Moscow, 119333 Russia
*e-mail: dymnikov@inm.ras.ru
**e-mail: pperezhogin@gmail.com

Abstract—Statistical properties of different finite-dimensional approximations of two-dimensional ideal fluid equations are studied. A special class of approximations introduced by A.M. Obukhov (systems of hydrodynamic type) is considered. Vorticity distributions over area and quasi-equilibrium coherent structures are studied. These coherent structures are compared to structures occurring in a viscous fluid with random forcing.

1. INTRODUCTION

The problem of studying two-dimensional turbulence is very important in geophysical fluid dynamics, since the atmosphere and ocean are quasi-two-dimensional. There are two key problems in geophysical fluid dynamics: weather forecasting and climate-change forecasting. From the mathematical standpoint, the first problem is related to studying the behavior of a solution to a system on a finite time interval. To justify this problem, it suffices to have global solvability theorems and theorems of convergence of solutions to finite-dimensional approximations to a solution to the differential problem. Theorems of this type exist for the two-dimensional ideal and viscous fluid equations [2, 9, 20, 24]. However, constants of convergence (if they are defined), as a rule, exponentially depend on the time interval on which the problem is studied; when this interval tends to infinity, these theorems lose their meaning. These situations arise when we study climate simulation problems on an arbitrarily long time interval. Therefore, the problem of studying the two-dimensional fluid dynamics on an arbitrarily long time interval is a key problem in climate theory. Clearly, these dynamics are different for a viscous fluid (dynamics on an attractor) and an ideal fluid. In the asymptotic case, when we study the two-dimensional fluid dynamics for a very small viscosity (the so-called decaying turbulence), the two-dimensional fluid behaves on sufficiently long time intervals like an ideal fluid (see, for example [7, 8, 14, 26]).

In real problems of weather forecasting and climate theory, we deal with a quasi-two-dimensional fluid with forcing and dissipation; from this standpoint, two-dimensional ideal fluid problems seem to be quite academic. However, this is far from the case: we should bear in mind that, for example, there are so-called inertial ranges in simulated energy distributions over the spectrum, in which the dissipation and forcing are small and the fluid behaves like an ideal one [17]. The characteristic features of the behavior of an ideal fluid can also be observed in other characteristics of a viscous fluid, on which we dwell below. From this point of view, studying the ideal fluid dynamics is not only an academic problem, but also a problem that is essentially useful in practice. Since the practical problems of weather forecasting and climate theory can be solved only numerically, the problem of studying the properties of finite-dimensional approximations of the original differential problem is very important [10, 15, 18, 28]. When studying approximations of the two-dimensional ideal fluid equations, the condition that these approximations belong to the class of systems of hydrodynamic type is natural (in addition to the approximation—stability condition). Recall that, in [6], Obukhov called a finite-dimensional system

$$\frac{du_i}{dt} = F_i(u), \ u|_{t=0} = u^0 \tag{1.1}$$

with respect to the unknown $u = [u_1, u_2, ..., u_n]$ a system of hydrodynamic type if it satisfies the following three requirements:

(1) System (1.1) is quadratically nonlinear;

(2) The phase flow is incompressible:

$$\sum_i \frac{\partial F_i}{\partial u_i} = 0;$$

and

(3) The system has at least one quadratic conservation law $(Su, u) = \text{const}$, where S is a positive definite symmetric matrix.

The problem that we deal with in this work is studying the statistical properties of finite-dimensional approximations of the equations describing the two-dimensional ideal fluid dynamics that belong to the class of system of hydrodynamic type in the sense of the above definition.

Prior to giving a specific statement of the problem, we briefly dwell on the fundamental properties of the systems of equations describing the two-dimensional ideal fluid dynamics. We write the original equations of the two-dimensional ideal incompressible fluid dynamics in terms of vorticity and the stream function:

$$\frac{\partial \omega}{\partial t} + J(\psi, \omega) = 0, \qquad (1.2)$$

where $\omega = \Delta \psi$ is vorticity, ψ is the stream function, and $J(\psi, \omega) = -\dfrac{\partial \psi}{\partial y}\dfrac{\partial \omega}{\partial x} + \dfrac{\partial \psi}{\partial x}\dfrac{\partial \omega}{\partial y}$ is the Jacobian. We consider system (1.2) in a doubly periodic channel D in the Cartesian system of coordinates; thus, we have $\int_D \omega dD = 0$. It is well known [4] that system (1.2) has the energy conservation law

$$E = -\frac{1}{2}\int_D \psi \omega dD = \text{const}, \qquad (1.3)$$

and infinitely many invariants (Casimirs) of the form

$$\int_D F(\omega) dD = \text{const}. \qquad (1.4)$$

If we assume that $F(\omega) = \dfrac{1}{2}\omega^2$, then we have the enstrophy conservation law

$$\overline{\omega^2} = \frac{1}{2}\int_D \omega^2 dD = \text{const}. \qquad (1.5)$$

It follows from (1.3) and (1.5) that we have the law of conservation of the energy-averaged squared wavenumber:

$$\overline{k^2} = \frac{\overline{\omega^2}}{E} = \text{const}. \qquad (1.6)$$

Infinitely many conservation laws (1.4) are equivalent to the preservation of the vorticity distribution over area [25], which is given by the formula

$$\frac{dD}{D} = \rho(\omega) d\omega; \qquad (1.7)$$

that is, $\rho(\omega)$ is an invariant. Provided that we introduce the notion of information entropy [5], it follows that the entropy

$$S = -\int_{-\infty}^{+\infty} \rho \ln \rho \, d\omega, \rho \equiv \rho(\omega) \qquad (1.8)$$

is an invariant as well.

Since any finite-dimensional approximation, even one belonging to the class of systems of hydrodynamic type, cannot have infinitely many invariants, studying the behavior of the density of the vorticity distribution over area $\rho(\omega)$ is a very interesting and promising problem for not only an ideal fluid, but also the real atmosphere [5].

We need another definition of entropy [13]; that is,

$$S = -\int_D dD \int_{-\infty}^{+\infty} \rho \ln \rho \, d\omega, \ \ \rho \equiv \rho(x, y, \omega), \qquad (1.9)$$

where $\rho(x, y, \omega)$ is used to specify an ensemble in the RSM mean field theory [21, 23] and denotes the distribution over an area that depends on the spatial point. Reviews of the RSM theory are given in [7, 13].

Now we consider other characteristics of a quasi-equilibrium state of an ideal two-dimensional fluid. These characteristics were studied by different authors [10, 14, 26, 28]. According to the RSM theory, the energy in a quasi-equilibrium state is concentrated in a large-scale coherent structure determined by a stationary solution to system (1.2):

$$\overline{\omega} = F(\overline{\psi}), \qquad (1.10)$$

where the upper line denotes the removal of small-scale flow components. If we use the variational principle of maximization of entropy (1.9) at a given energy E and an enstrophy $\overline{\omega^2}$, then function F is linear with the slope, corresponding to the minimum (in modulus) eigenvalue of the Laplace operator $\lambda_{\min}$ [13]:

$$\triangle \psi_1 = -|\lambda_{\min}|\psi_1. \qquad (1.11)$$

Since the condition

$$\frac{\partial F}{\partial \overline{\psi}} > -|\lambda_{\min}|,$$

is a sufficient condition for a stationary solution to be stable [4], we can conclude that the stability criterion for a condensed stationary solution (1.11) corresponds in this case to the limit point of the stability test.

According to the point vortex model [27], relation (1.10) has the form

$$\overline{\omega} = \alpha \sinh(\beta \overline{\psi}), \qquad (1.12)$$

which also yields that the relation between $\overline{\omega}$ and $\overline{\psi}$ is linear for small values of the stream function (large scales).

Therefore, the main problems considered in this study are the following problems:

(1) Studying the vorticity distribution over an area reproduced by different approximations of the two-dimensional ideal incompressible fluid equations that belong to the class of systems of hydrodynamic type;

(2) Studying the quasi-equilibrium coherent structures reproduced by these finite-dimensional approximations;

(3) Comparing these coherent structures to structures generated by a viscous fluid with random forcing.

2. DIFFERENCE SCHEMES AND PROBLEM-SOLVING METHODS

As a subject of study, we take three difference schemes approximating Eq. (1.2) and belonging to the class of systems of hydrodynamic type. The schemes are constructed based on different representations of the Jacobian $J(\psi, \omega)$ (see [7, 22] for a detailed description of different methods for constructing the schemes for (1.2)). It is well known that the Jacobian J can be written in three representations:

$$J_1 = \frac{\partial \psi}{\partial x}\frac{\partial \omega}{\partial y} - \frac{\partial \psi}{\partial y}\frac{\partial \omega}{\partial x} \qquad (2.1)$$

—is the flow form,

$$J_2 = \frac{\partial}{\partial y}\left(\frac{\partial \psi}{\partial x}\omega\right) - \frac{\partial}{\partial x}\left(\frac{\partial \psi}{\partial y}\omega\right) \qquad (2.2)$$

—is the first divergence form,

$$J_3 = \frac{\partial}{\partial x}\left(\frac{\partial \omega}{\partial y}\psi\right) - \frac{\partial}{\partial y}\left(\frac{\partial \omega}{\partial x}\psi\right) \qquad (2.3)$$

—is the second divergence form.

Based on these three forms, we can construct spatial approximations preserving the enstrophy, energy, and energy and enstrophy (the Arakawa scheme [11]) by using symmetric approximations of the derivatives on a uniform mesh. The phase-flow preservation for these approximations was proved in [15].

The E scheme preserving the energy has the form

$$J^h = \frac{1}{2}[J_1^h(\psi_h, \omega_h) + J_3^h(\psi_h, \omega_h)], \qquad (2.4)$$

where J_1^h and J_3^h are approximations of J_1 and J_3.

The Z scheme preserving the enstrophy has the form

$$J^h = \frac{1}{2}[J_1^h(\psi_h, \omega_h) + J_2^h(\psi_h, \omega_h)], \qquad (2.5)$$

and the ZE scheme preserving the energy and enstrophy has the form

$$J^h = \frac{1}{3}[J_1^h(\psi_h, \omega_h) + J_2^h(\psi_h, \omega_h)) + J_3^h(\psi_h, \omega_h)]. \qquad (2.6)$$

We can easily show that, if the Crank–Nicolson scheme is used with spatial approximations (2.4), (2.5), and (2.6) to approximate Eq. (1.2), then all the conservation laws mentioned above hold at each step in time. The resulting procedure of time integration consists of solving the system of nonlinear algebraic equations with a quadratic nonlinearity of the form

$$\frac{\omega_h^{n+1} - \omega_h^n}{\Delta t} + J^h\left(\frac{\psi_h^{n+1} + \psi_h^n}{2}, \frac{\omega_h^{n+1} + \omega_h^n}{2}\right) = 0, \qquad (2.7)$$

where n denotes the number of the time layer. To find a numerical solution to this system, we use the method of simple iterations, which is described in [7] in detail. The number of iterations is 5, and this ensures the preservation of the quadratic invariants with a relative accuracy of 10^{-4} to 10^{-3}.

3. RESULTS OF NUMERICAL EXPERIMENTS WITH SCHEMES APPROXIMATING THE IDEAL FLUID EQUATIONS

Prior to discussing the results of numerical experiments, we make several observations.

(1) For infinite-dimensional spaces (differential statement of the problem), we have an analog of the embedding theorem [4]

$$E = -\frac{1}{2}(\psi, \omega) \leq \frac{1}{|\lambda_{\min}|}\frac{(\omega, \omega)}{2} \equiv \frac{1}{|\lambda_{\min}|}\overline{\omega^2},$$

where $\lambda_{\min}$ is the modulus-minimum eigenvalue of the Laplace operator. For a finite-dimensional space, in the case of a uniform square mesh, we can obtain the relations between the energy and enstrophy in the following way. Let

$$E_h = -\frac{1}{2}(\psi_h, \omega_h)_h, \overline{\omega_h^2} = \frac{1}{2}(\omega_h, \omega_h)_h,$$

where $(\cdot, \cdot)_h$ is a scalar product in a finite-dimensional space. Let S_h be a symmetric negative definite approximation of the Laplace operator. We consider a pair of subspaces that are constant orthogonal, that is, $(\omega_h, 1)_h = 0$ and $(\psi_h, 1)_h = 0$, on which the action of S_h is one-to-one. Then we have $\omega_h = S_h \psi_h$ and $\psi_h = S_h^{-1}\omega_h$. Hence, we obtain a two-sided estimate of the energy level

$$\frac{1}{|\lambda_{\max}^h|}\overline{\omega_h^2} \leq E_h \leq \frac{1}{|\lambda_{\min}^h|}\overline{\omega_h^2}, \qquad (3.1)$$

where the eigenvalues of the matrix S_h depend on the parameters of the problem as follows:

$$\left|\lambda_{\max}^h\right| = \frac{\alpha}{h^2}, \alpha = \text{const}, \, h \text{ is the mesh step,}$$

$$\left|\lambda_{\min}^h\right| = \beta, \beta \text{ is a constant determined by the size of the domain.}$$

Thus, when we consider the scheme preserving only the enstrophy, the energy is bounded from above by a constant independent of the mesh step:

$$E_h \leq \frac{1}{\beta} \overline{\omega_h^2}. \tag{3.2}$$

In this case, the generation of energy, if it occurs, proceeds on large scales, since the mean square of the wavenumber $\overline{k_h^2} = \frac{\overline{\omega_h^2}}{E_h}$ has to decrease. In addition, the almost complete dissipation of energy is possible [15].

When we consider the scheme preserving only the energy, the enstrophy satisfies the relation

$$\overline{\omega_h^2} \leq \frac{\alpha}{h^2} E_h. \tag{3.3}$$

This relation means that the mean square of the wavenumber $\overline{k_h^2} = \frac{\overline{\omega_h^2}}{E_h} \leq \frac{\alpha}{h^2}$ can unboundedly increase as $h \to 0$; that is, an energy cascade toward high wavenumbers can occur in this scheme.

(2) The relations corresponding to the modulus-minimum eigenvalue of the Laplace operator acting on functions defined on a doubly periodic channel are degenerate, since the two-dimensional eigenspace corresponds to this eigenvalue. This means that the form of the coherent structure formed on this subspace is not defined unambiguously.

(3) Generally speaking, the results of quasi-equilibrium distributions depend on the configuration of the initial state, in particular, on the average wavenumber [18]. If we specify the initial state so that $\overline{k^2} = \overline{\omega^2}/E \gg |\lambda_{\min}(\Delta)|$, then, as was shown in numerous works [7, 15, 28], quasi-equilibrium distributions over area for systems of hydrodynamic type are determined by fluctuations with respect to the average state. This distribution has to be close to a normal one [7], which also follows form the fact that entropy (1.8) is maximized on a normal distribution if there is a quadratic invariant (see, for example, [19]).

(4) The convergence to a quasi-equilibrium state in a system of hydrodynamic type should occur if the definition of convergence includes filtering, for example, averaging over space $\overline{\omega}$ (we will average over the cells consisting of $n \times n$ calculation points) or averaging over time $\langle \omega \rangle = \frac{1}{T} \int_0^T \omega dt$ (Cesáro convergence). The theory of Cesáro convergence is described in

detail in [1]. We will always indicate which procedure is used in our numerical experiments.

(5) We studied the Arakawa scheme (*ZE*) in detail in [7]. It was shown in this work that the scheme is equivalent in its properties to the Galerkin method with eigenfunctions of the Laplace operator as its basis functions.

Numerical experiments have been performed with the following parameters for all the schemes (*E*, *Z*, and *ZE*). The doubly periodic channel *D* has the size $[0, 2\pi] \times [0, 2\pi]$, and the resolution of the calculation mesh is 512×512 points. The initial vorticity field consists of 8×8 square sections in which the vorticity is constant and randomly takes a value from the set $\{-1 + a, -1 + 3a, \ldots, 1 - a\}$, $a = 1/64$; each value is selected exactly once. Similar initial data were used in [7, 8]. The mean square of the wavenumber for these initial data is $\overline{k^2} = \overline{\omega^2}/E = 4.4 > |\lambda_{\min}(\Delta)| = 1$. The calculation has been performed for the long time interval $t \in (0, 50\,000)$. A complete statistical equilibrium for all the schemes occurs no later than at the moment $t \approx 10\,000$.

First we give the results for the scheme with two invariants (the *ZE* scheme); thereafter, we compare this scheme to the other two schemes (the *Z* and *E* schemes).

In the calculation with the *ZE* scheme, the energy and enstrophy are preserved with a relative accuracy of 10^{-4} for the entire calculation time (Figs. 1a, 1b). Figure 2 shows the vorticity distribution over area $\rho(\omega)$ at the last time moment. It can be seen from Fig. 2 that the distribution has a Gaussian form. The variance of the distribution is determined by the initial data and is $2\overline{\omega^2}/D$. We use the kurtosis $\gamma = \frac{\int \omega^4 \rho d\omega}{\left(\int \omega^2 \rho d\omega\right)^2}$ to determine the closeness of the distribution over area $\rho(\omega)$ to a Gaussian distribution ($\gamma = 3$ for the standard normal distribution). Figure 3 shows the kurtosis as a function of time for three distinct resolutions (a standard resolution of 512×512 and two more resolutions of 128×128 and 2048×2048). This coefficient grows abruptly on the time interval $t \in (0, 50)$, which is related to the onset of statistical equilibrium in small scales. Thereafter, on the long time interval $t \in (50, 10\,000)$, the large scales also come to a complete statistical equilibrium, and the kurtosis becomes almost 3 for all the resolutions (this is not shown in Fig. 3). As a typical time of equilibrium onset in small scales, we take
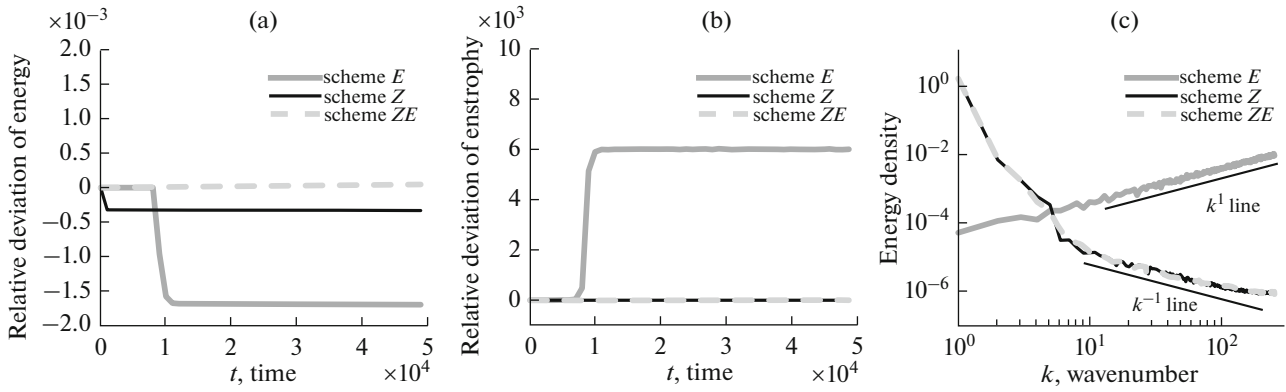
Fig. 1. Relative deviations of (a) energy and (b) enstrophy from the initial values and (c) the spectral energy distribution at the last time moment $t = 50000$ for three schemes (E, Z, and ZE). Pay attention, the scales of (a) and (b) differ by 6 orders of magnitude.
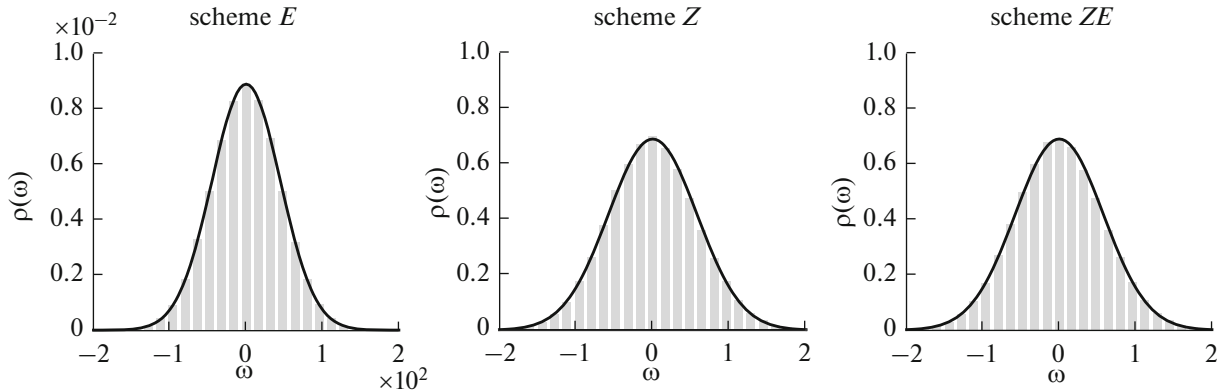

Fig. 2. Histogram of the vorticity distribution over area at the last time moment $t = 50000$ for three schemes (E, Z, and ZE). The number of intervals of the histogram is 25. The black curve shows a Gaussian distribution with an equivalent variance.

the time during which the kurtosis attains a value of 3 for the first time. The typical time slowly grows with increasing resolution ($T \sim N^{0.3}$, where N is the number of mesh points along one direction) (see Fig. 3). This is an illustration of the convergence theorem: the higher the resolution of the calculation mesh is, the longer the time during which the initial distribution $\rho(\omega)$ is preserved.

Now we describe the properties of a statistical equilibrium state for the Arakawa ZE scheme. It follows from the theory that the enstrophy in small scales has to be equipartitioned among the Fourier harmonics [7]. This fact is confirmed by the numerical experiment: the energy spectrum has a decreasing power law $E(k) \sim k^{-1}$ in small scales (see Fig. 1c). It also follows from Fig. 1c that most energy accumulates in large scales, which results in the formation of large-scale coherent structures with a typical size comparable to the size of the domain (see Fig. 4). Two large vortices are formed by the time moment $t \approx 200$, which is followed by slow processes of establishing the statistical

equilibrium. Large vortices are close to stationary solutions of the ideal fluid equations: the $\langle \psi \rangle - \langle \omega \rangle$ scatter plot is described by a functional dependence (see Fig. 5). This functional dependence is close to linear dependence (1.11); for large values of the stream function, there are deviations from the linear dependence, thus qualitatively confirming formula (1.12).

Unlike [7], we used time averaging to isolate coherent structures (Cesáro convergence). This became possible due to the fact that the initial data taken by us lead to more stationary quasi-equilibrium states: the drift of large-scale vortices is insignificant.

The scheme with enstrophy as the only quadratic invariant (the Z scheme) gives results similar to the results of the ZE scheme (Figs. 1, 2, 4, 5). In this case, the energy is approximately preserved during the entire calculation time (see Fig. 1a). A similar result is described in [12]. Note that other systems of hydrodynamic type with invariant enstrophy can dissipate the energy, and no coherent structure occurs [15]. In addition, the generation of energy is possible.
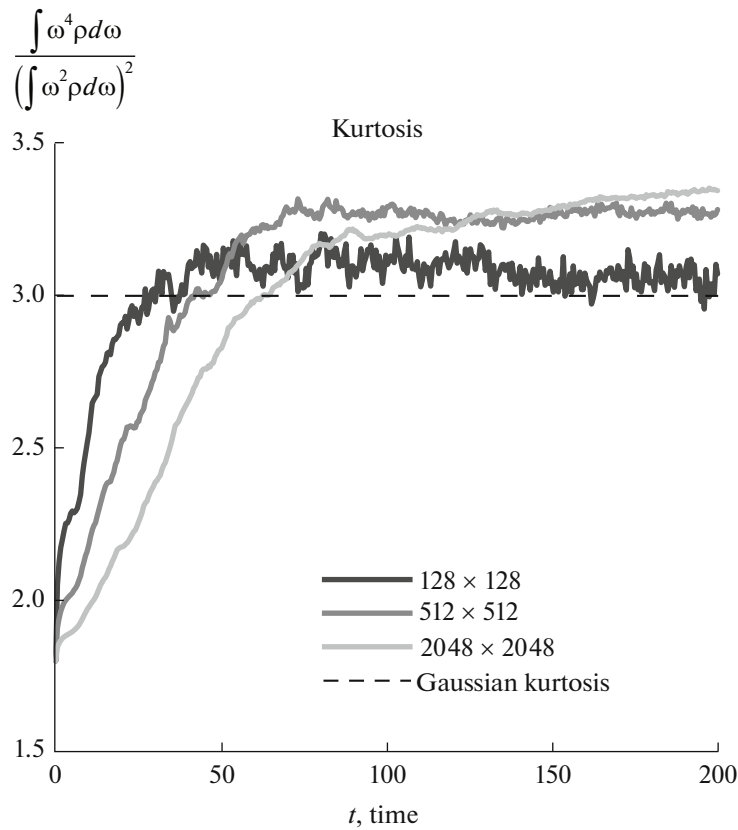
$$\frac{\int \omega^4 \rho \, d\omega}{\left(\int \omega^2 \rho \, d\omega\right)^2}$$

Fig. 3. Kurtosis of the distribution $\rho(\omega)$ for calculations using the *ZE* scheme with three different resolutions.
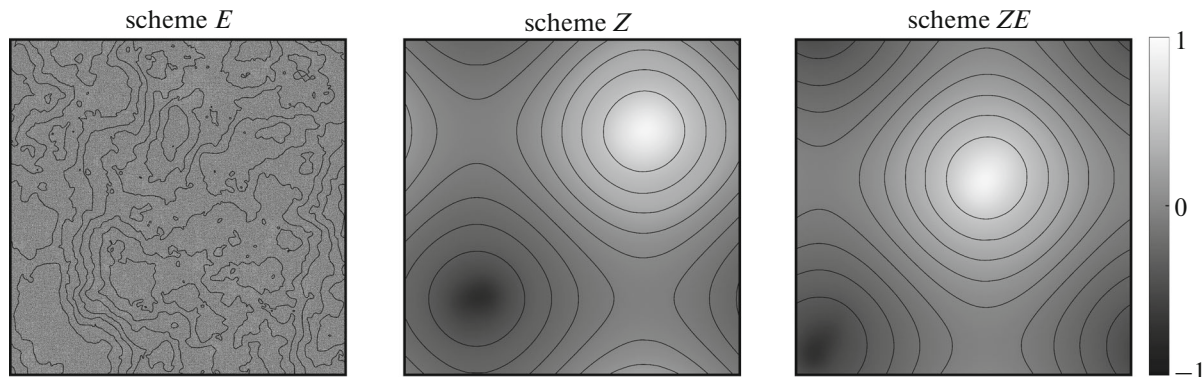

Fig. 4. Vorticity (shown by color) and the stream function (shown by lines) averaged preliminarily over the time interval $t \in (20\,000,\ 50\,000)$.

We studied a system of this type but do not give detailed results here.

As was shown above, the scheme with energy as the only quadratic invariant (the *E* scheme) can unlimitedly generate the enstrophy. This is the case in the numerical experiment: the enstrophy level increases by a factor of 6000 during the onset of statistical equilibrium (see Fig. 1b). The excess enstrophy accumulates in small scales; this results in the fact that the energy cascades into the region of high wavenumbers, where the energy is equipartitioned among the Fourier harmonics (after integrating over the angle in the Fourier space, $E(k) \sim k$) (see Fig. 1c). Consequently, coherent structures are not formed on large scales (Figs. 4, 5). Due to the generation of enstrophy, the variance of the distribution over area $\rho(\omega)$ increases significantly when compared to the *ZE* and *Z* schemes (see Fig. 2). The functional form of the distribution does not change: its remains Gaussian.
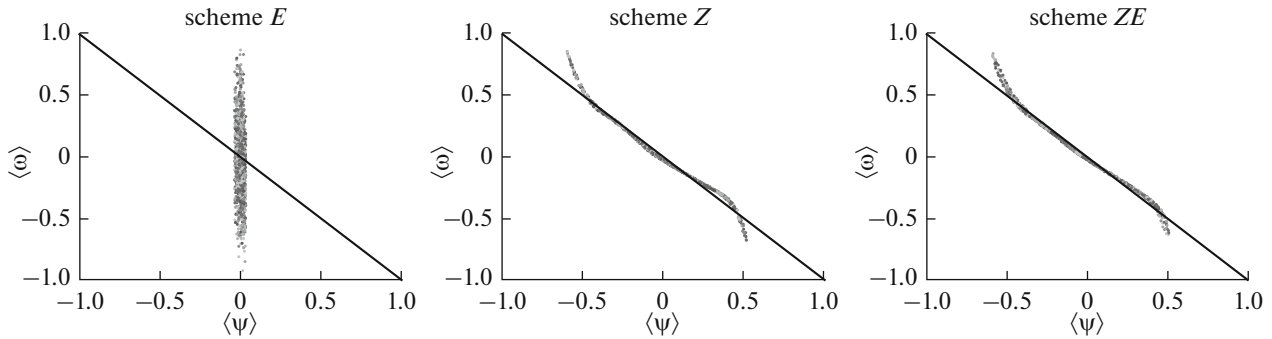
Fig. 5. The $\langle\psi\rangle - \langle\omega\rangle$ scatter plot where the angle brackets denote the averaging over the time interval $t \in (0, 50\,000)$. The black line corresponds to the relation $\langle\omega\rangle = -\langle\psi\rangle$: prediction of the theory (1.11) with allowance for $|\lambda_{min}| = 1$.

4. LARGE-SCALE STRUCTURE AND THE VORTICITY DISTRIBUTION OVER AREA IN TWO-DIMENSIONAL EQUATIONS WITH DISSIPATION AND FORCING

We consider two-dimensional viscous fluid equations in a doubly periodic channel:

$$\frac{\partial\omega}{\partial t} + J(\psi,\omega) = f - \alpha\omega + \mu\Delta\omega,$$

$$\omega|_{t=0} = \omega^0,$$ (4.1)

where $\omega = \Delta\psi$, f is external forcing, α is the Rayleigh friction coefficient, and μ is the coefficient of viscosity. The asymptotic properties of this equation were studied in numerous works (see [4] and the references therein). Let

$$\frac{\partial\omega_h}{\partial t} + J^h(\psi_h,\omega_h) = f_h - \alpha\omega_h + \mu\Delta_h\omega_h,$$

$$\omega_h|_{t=0} = \omega_h^0,$$ (4.2)

be a finite-difference approximation of (4.1) in which system (4.2) with $f = 0$, and $\alpha = 0$, $\mu = 0$ is a system of hydrodynamic type. The central question considered by us in this section is as follows: In what sense are the asymptotic (statistical) properties of (4.2) determined by the asymptotic (statistical) properties of the corresponding system of hydrodynamic type?

The equations for energy and enstrophy in system (4.1) have the form

$$\frac{\partial E}{\partial t} = -(f,\psi) - 2\alpha E - 2\mu\overline{\omega^2},$$ (4.3)

$$\frac{\partial\overline{\omega^2}}{\partial t} = (f,\omega) - 2\alpha\overline{\omega^2} + \mu(\Delta\omega,\omega).$$ (4.4)

Averaging (4.3) and (4.4) over time, we obtain the average values of energy $\langle E\rangle$ and enstrophy $\langle\overline{\omega^2}\rangle$:

$$\langle E\rangle = \frac{-\langle(f,\psi)\rangle - 2\mu\langle\overline{\omega^2}\rangle}{2\alpha},$$ (4.5)

$$\langle\overline{\omega^2}\rangle = \frac{\langle(f,\omega)\rangle + \mu\langle(\Delta\omega,\omega)\rangle}{2\alpha}.$$ (4.6)

Relations (4.5) and (4.6) express the principal difference between systems (1.2) and (4.1): in the first case, $\langle E\rangle$ and $\langle\overline{\omega^2}\rangle$ are determined by the initial data; in the second case, these values do not depend on the initial data (in the asymptotics). When solving Eqs. (4.1), it is useful to use schemes that prevent the growth of enstrophy. According to (4.5), an increase in the level of enstrophy results in a reduction in the level of energy and, consequently, in the growth of the mean square of the wavenumber. This effect was demonstrated in [22], where we thoroughly studied the energy distribution over the spectrum for different schemes of solving Eqs. (4.1).

As for an ideal fluid, we are interested in characteristics of system (4.1) such as large-scale coherent structures and the vorticity distribution over area. Let the forcing be given on spatial scales so that two inertial ranges can be formed. In these ranges, by definition, the dissipation should not significantly affect the formation of the energy distribution over scales; that is, the fluid has to behave as an ideal fluid. We can achieve this by choosing the scale of dissipation due to viscosity much less than the forcing scale and the time scale of the Rayleigh friction much larger than the time scale of energy transfer over the spectrum. The first condition is satisfied for sufficiently small coefficients μ. It was shown in [7] that, for sufficiently small μ, quasi-equilibrium states of a dissipative fluid are close to the corresponding states of an ideal fluid, excepting the vorticity distribution over the scales close to the dissipation scale.

Further, we can obtain from dimensional analysis that the typical time of energy transfer over the spectrum is $\tau \sim k^{-3/2}E(k)^{-1/2}$, where k is the spatial wavenumber and $E(k)$ is the energy density in the wavenumber space. The Rayleigh dissipation becomes significant on the scale k_α on which the equality $1/\alpha = \tau$ holds.
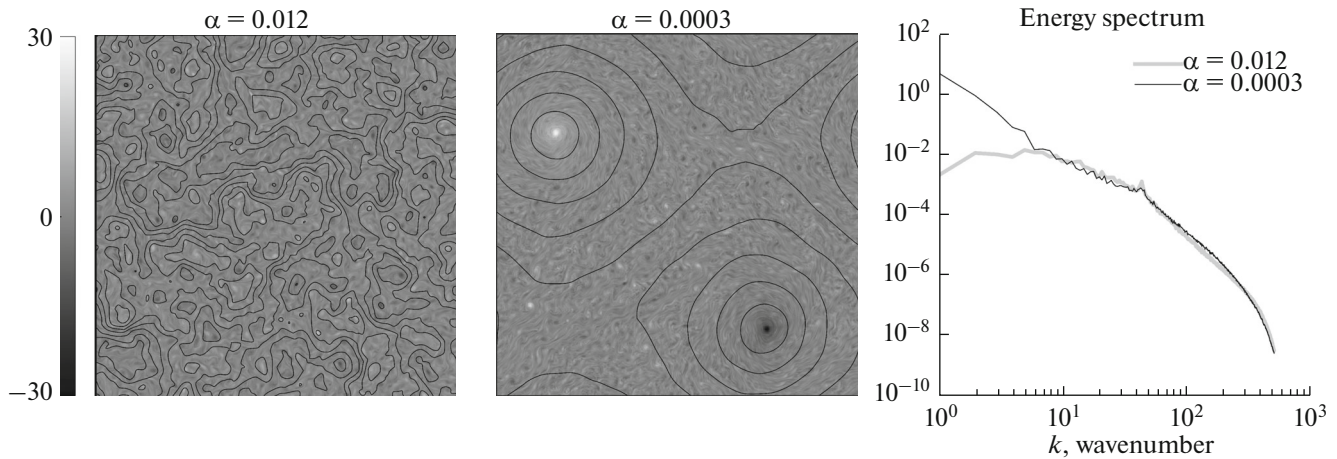
Fig. 6. Vorticity (shown by color) and the stream function (shown by lines) are on the left and the energy spectrum is on the right. The figures correspond to the last time moment $t = 15\,000$.

Taking account of the fact that the distribution $E(k) \sim k^{-5/3}$ is the case for an inverse energy cascade, we arrive at the estimate

$$k_\alpha \sim \alpha^{3/2}; \qquad (4.7)$$

a similar estimate is given in [3]. On this scale, the cascade is blocked. For the energy in the inverse cascade to reach scales comparable to the typical scale of the domain, the coefficient α should be made sufficiently small. Then, with fixed μ and f, the average energy attains high values. If α tends to 0, then we can easily obtain that

$$E^{1/2} \le \frac{\sqrt{2}}{2} \frac{\|f\|}{\mu \, |\lambda_{\min}(\Delta)|^{3/2}}, \qquad (4.8)$$

where $\lambda_{\min}(\Delta)$ is the modulus-minimum eigenvalue of the Laplace operator.

We performed two numerical experiments for problem (4.1), which we solved by the Arakawa *ZE* scheme, with the following parameters (all the parameters are made dimensionless [22]): a resolution of 1024×1024, the δ-correlated random forcing is given at a wavenumber of 45 and provides energy input per unit area and unit time at the level of $\varepsilon = 1.5 \cdot 10^{-4}$, $\mu = 4.69 \times 10^{-6}$, and the calculation time is $t = 15\,000$. The difference between the experiments lies in choosing the Rayleigh friction coefficient: $\alpha = 0.012$ and $\alpha = 0.0003$. According to (4.7), the scale of energy cascade blocking in these experiments should differ by a factor of 253.

Figure 6 shows the energy distribution over the spectrum in the two experiments. It can be seen from Fig. 6 that, with a large Rayleigh friction coefficient of $\alpha = 0.012$, the energy cascade into the regions of low wavenumbers is blocked at the wavenumber $k_\alpha = 5$; in this case, there is no quasi-stationary coherent structure. With a small Rayleigh friction coefficient of $\alpha = 0.0003$, there are already coherent structures close to those occurring in an ideal fluid (cf. Figs. 4, 6). The $\overline{\psi} - \overline{\omega}$ scatter plot is given in Fig. 7. As in an ideal fluid, with a small Rayleigh friction, there is a functional dependence $\overline{\omega} = F(\overline{\psi})$ that is close to linear dependence (1.11) for small $\overline{\psi}$ and to a function of the form sinh (1.12) for large $\overline{\psi}$. In both cases, the vorticity distribution over area is close to a Gaussian distribution (see Fig. 7). It is worth noting that vorticity distributions over area that are close to Gaussian distributions also occur when calculating with real atmospheric data (the 500 mb surface) [5].

5. DISCUSSION OF THE RESULTS AND CONCLUSIONS

In this work we studied the statistical properties of three difference schemes approximating the two-dimensional ideal incompressible fluid equations and belonging to the class of systems of hydrodynamic type introduced by Obukhov. These systems were approximated in time so that the quadratic conservation laws accurately hold in the case of accurate arithmetic. It was shown that, even with a convergence theorem on a finite time interval for one of the difference schemes (the Arakawa scheme with two quadratic invariants being the energy and enstrophy), the schemes basically cannot reproduce some properties of a two-dimensional ideal fluid when we consider an arbitrarily large time interval. In particular, this concerns the preservation of the vorticity distribution over area, the reproduction of which requires infinitely many invariants (Casimirs). The time interval on which the initial vorticity distribution over area is approximately preserved increases slowly with increasing resolution, which nevertheless agrees with the convergence theorem.
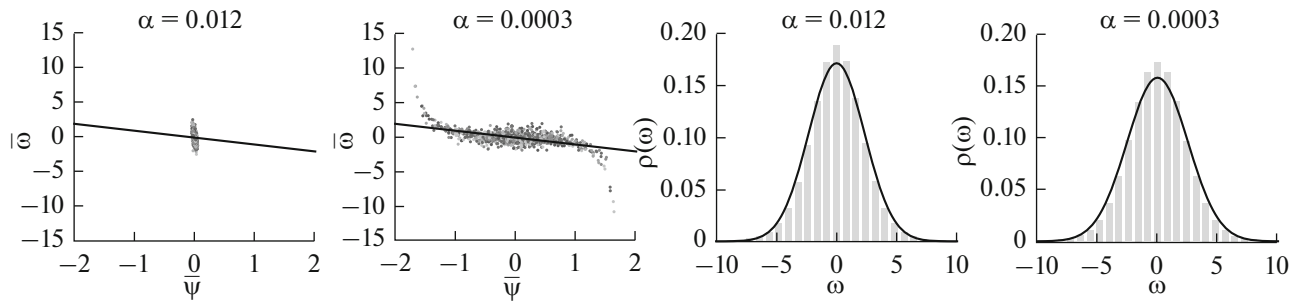
Fig. 7. The $\overline{\psi} - \overline{\omega}$ scatter plot where the upper line denotes the averaging over cells of 32×32 calculation points, is on the left; the black line corresponds to linear relation (1.11). The distribution over area is on the right; the number of intervals of the histogram is 25, and the black line shows a Gaussian distribution with an equivalent variance. The figures correspond to the last time moment $t = 15\,000$.

The scheme preserving only the energy does not reproduce other important properties of an ideal fluid, in particular, the formation of a stationary quasi-equilibrium state satisfying a linear relation between the vorticity and the stream function when performing a certain averaging (for example, considering the Cesáro convergence) and the energy distribution over the spectrum. As for the scheme preserving only one quadratic invariant being the enstrophy, the results of a simulation of quasi-equilibrium states of an ideal fluid using it differ little from the results obtained by the Arakawa scheme, which can be explained by the existence of an embedding theorem preventing an energy cascade toward high wavenumbers.

The following question arises: Is it necessary to take into account the reproduction of the fundamental properties of a two-dimensional ideal fluid when simulating a quasi-two-dimensional viscous fluid with external forcing? For a viscous fluid, we have a global solvability theorem and theorems of convergence of solutions of difference schemes to solutions of differential problems that have the only quadratic invariant being the energy when the coefficient of viscosity and forcing tend to zero (a bad scheme from the standpoint of reproducing the statistical properties of an ideal fluid). However, it should be noted that constants in all these theorems (if they are defined), as a rule, exponentially depend on the time interval; thus, the theorems almost cannot help us in studying the above problem. We can reformulate this problem in terms of studying the properties of an invariant measure on an attractor of the system; however, in this statement, the problem does not become simpler. It is physically clear that, when we deal with a mesh of a high spatial resolution so that inertial ranges (where the fluid behaves like an ideal fluid, since the dissipation and forcing in these regions can be neglected) occur in the energy distribution over the spectrum, the answer to this question is positive (at least for an inertial range in which a direct enstrophy cascade occurs). For a range in which an inverse energy cascade proceeds (we assume that the external action is on middle wave-numbers), there is another problem related to the Rayleigh friction, which blocks the inverse energy cascade when the typical time of friction is close to the typical time of the energy cascade over the spectrum in the interval of blocking. We have shown in this study that, for small Rayleigh friction coefficients, large-scale coherent structures do occur; for large coefficients, there are no structures of this type. This problem can be important when external forcing compensates the Rayleigh friction completely or in part. This hypothesis has the right to life, for example, when studying large-scale blocking cases [16].

REFERENCES

1. V. V. Kozlov, *Gibbs Ensembles and Nonequilibrium Statistical Mechanics* (Institut komp'yuternykh issledovanii, Moscow−Izhevsk, 2008) [in Russian].
2. V. F. Baklanovskaya, "Analysis of the method of grids for 2D Navier−Stokes type equations with nonnegative viscosity. II," Zh. Vychisl. Mat. Mat. Fiz. **24** (12), 1827−1841 (1984).
3. S. D. Danilov and D. Gurarie, "Quasi-two-dimensional turbulence," Phys.-Usp. **43** (9), 863−900 (2000).
4. V. P. Dymnikov, *Stability and Predictability of Large-Scale Atmospheric Processes* (IVM RAN, Moscow, 2007) [in Russian].
5. V. P. Dymnikov, E. V. Kazantsev, and V. V. Kharin, "Informational entropy and local Lyapunov exponents of barotropic atmospheric circulation," Izv. Akad. Nauk, Fiz. Atmos. Okeana **28** (6), 563−573 (1992).
6. A. M. Obukhov, "On integral invariants in hydrodynamic-type systems," Dokl. Akad. Nauk SSSR **184** (2), 309−312 (1969).
7. P. A. Perezhogin and V. P. Dymnikov, "Equilibrium states of finite-dimensional approximations of a two-

dimensional incompressible inviscid fluid," Nelinein-aya Din. **13** (1), 55−79 (2017).

8. P. A. Perezhogin and V. P. Dymnikov, "Modeling of quasi-equilibrium states of a two-dimensional ideal fluid," Dokl. Phys. **62** (5), 248−252 (2017).

9. V. I. Yudovich, "Nonstationary flows of an ideal incompressible liquid," Zh. Vychisl. Mat. Mat. Fiz. **3** (6), 1032−1066 (1963).

10. R. V. Abramov and A. J. Majda, "Statistically relevant conserved quantities for truncated quasigeostrophic flow," Proc. Nat. Acad. Sci. **100** (7), 3841−3846 (2003).

11. A. Arakawa, "Computational design for long-term numerical integration of the equations of fluid motion: Two-dimensional incompressible flow. Part I," J. Comput. Phys. **1** (1), 119−143 (1966).

12. A. Arakawa, *Design of the UCLA General Circulation Model* (Univ. of California, Dept. of Meteorology, Los Angeles, 1972), Tech. Rep. 7.

13. F. Bouchet and M. Corvellec, "Invariant measures of the 2D Euler and Vlasov equations," J. Stat. Mech.: Theory Exp., No. 8, P08021 (2010).

14. D. G. Dritschel, W. Qi, and J. Marston, "On the late-time behaviour of a bounded, inviscid two-dimensional flow," J. Fluid Mech. **783**, 1−22, (2015).

15. S. Dubinkina and J. Frank, "Statistical mechanics of Arakawa's discretizations," J. Comput. Phys. **227** (2), 1286−1305 (2007).

16. V. P. Dymnikov, "Instability indices for quasi-stationary atmospheric circulation regimes," Russ. J. Numer. Anal. Math. Modell. **5** (3), 189−198 (1990).

17. R. H. Kraichnan, "Inertial ranges in two-dimensional turbulence," Phys. Fluids **10** (7), 1417−1423 (1967).

18. R. H. Kraichnan, "Statistical dynamics of two-dimensional flow," J. Fluid Mech. **67** (1), 155−175 (1975).

19. J. H. C. Lisman and M. C. A. van Zuylen, "Note on the generation of most probable frequency distributions," Stat. Ned. **26** (1), 19−23 (1972).

20. C. Marchioro and M. Pulvirenti, *Mathematical Theory of Incompressible Nonviscous Fluids* (Springer, New York, 1994).

21. J. Miller, "Statistical mechanics of Euler equations in two dimensions," Phys. Rev. Lett. **65** (17), 2137−2140 (1990).

22. P. A. Perezhogin, A. V. Glazunov, E. V. Mortikov, and V. P. Dymnikov, "Comparison of numerical advection schemes in two-dimensional turbulence simulation," Russ. J. Numer. Anal. Math. Modell. **32** (1), 47−60 (2017).

23. R. Robert and J. Sommeria, "Statistical equilibrium states for two-dimensional flows," J. Fluid Mech. **229**, 291−310 (1991).

24. R. Robert, "On the statistical mechanics of 2D Euler equation," Commun. Math. Phys. **212** (1), 245−256 (2000).

25. R. Salmon, *Lectures on Geophysical Fluid Dynamics* (Oxford University Press, New York, 1998).

26. W. Qi and J. B. Marston, "Hyperviscosity and statistical equilibria of Euler turbulence on the torus and the sphere," J. Stat. Mech.: Theory Exp., No. 7, P07020 (2014).

27. A. Thess, J. Sommeria, and B. Juttner, "Inertial organization of a two-dimensional turbulent vortex street," Phys. Fluids **6** (7), 2417−2429 (1994).

28. A. Venaille, T. Dauxois, and S. Ruffo, "Violent relaxation in two-dimensional flows with varying interaction range," Phys. Rev. E **92** (1), 011001 (2015).

Translated by N. Berestova